Letter

Discovery and Preclinical Evaluation of BMS-711939, an Oxybenzyl-glycine Based PPAR# Selective Agonist

Yan Shi, Jun Li, Lawrence J Kennedy, Shiwei Tao, Andres S. Hernandez, Zhi Lai, Sean Chen, Henry Wong, Juliang Zhu, Ashok Trehan, Ngiap-Kie Lim, Huiping Zhang, Bang-Chi Chen, Kenneth T Locke, Kevin M O'Malley, Litao Zhang, Raiajit Srivastava, Bowman Miao, Daniel S. Meyers, Hossain Monshizadegan, Debra Search, Denise Grimm, Rongan Zhang, Thomas Harrity, Lori K Kunselman, Michael Cap, Jodi Muckelbauer, Chiehying Chang, Stanley R. Krystek, YiXin Li, Vinayak Hosagrahara, Lisa Zhang, Pathanjali Kadiyala, Carrie Xu, Michael A Blanar, Robert Zahler, Ranjan Mukherjee, Peter T.W. Cheng, and Joseph A Tino

ACS Med. Chem. Lett., **Just Accepted Manuscript** • DOI: 10.1021/acsmedchemlett.6b00033 • Publication Date (Web): 04 Apr 2016

	Zhang, Rongan; Bristol-Myers Squibb Pharmaceutical Research and Development Harrity, Thomas; Bristol-Myers Squibb Pharmaceutical Research and Development Kunselman, Lori; Bristol-Myers Squibb Pharmaceutical Research and Development Cap, Michael; Bristol-Myers Squibb Pharmaceutical Research and Development Muckelbauer, Jodi; Bristol-Myers Squibb Pharmaceutical Research and Development Chang, Chiehying; Bristol-Myers Squibb Pharmaceutical Research and Development Krystek, Stanley; Bristol-Myers Squibb, Computer-Assisted Drug Design Li, YiXin; Bristol-Myers Squibb Pharmaceutical Research and Development Hosagrahara, Vinayak; Bristol-Myers Squibb Pharmaceutical Research and Development Zhang, Lisa; Bristol-Myers Squibb Pharmaceutical Research and Development Kadiyala, Pathanjali; Bristol-Myers Squibb Pharmaceutical Research and Development Xu, Carrie; Bristol-Myers Squibb Pharmaceutical Research and Development Blanar, Michael; Bristol-Myers Squibb Pharmaceutical Research and Development Zahler, Robert; Bristol-Myers Squibb Pharmaceutical Research and Development Mukherjee, Ranjan; Bristol-Myers Squibb Pharmaceutical Research and Development Cheng, Peter; Bristol-Myers Squibb Pharmaceutical Research Institute, Metabolic Diseases Chemistry Tino, Joseph; Bristol-Myers Squibb Pharmaceutical Research and Development

Discovery and Preclinical Evaluation of BMS-711939, an Oxybenzyl-glycine Based PPARα Selective Agonist

Yan Shi,* Jun Li, Lawrence J. Kennedy, Shiwei Tao, Andrés S. Hernández, Zhi Lai, Sean Chen, Henry Wong, Juliang Zhu, Ashok Trehan, Ngiap-Kie Lim, Huiping Zhang, Bang-Chi Chen, Kenneth T. Locke, Kevin M. O'Malley, Litao Zhang, Raiajit Srivastava, Bowman Miao, Daniel S. Meyers, Hossain Monshizadegan, Debra Search, Denise Grimm, Rongan Zhang, Thomas Harrity, Lori K. Kunselman, Michael Cap, Jodi Muckelbauer, Chiehying Chang, Stanley R. Krystek, Yi-Xin Li, Vinayak Hosagrahara, Lisa Zhang, Pathanjali Kadiyala, Carrie Xu, Michael A. Blanar, Robert Zahler, Ranjan Mukherjee, Peter T. W. Cheng, Joseph A. Tino

Research and Development, Bristol-Myers Squibb Company, 350 Carter Road, Hopewell, NJ 08540, U.S.A.

KEYWORDS: peroxisome proliferator-activated receptor (PPAR) α selective agonist, high fat fed hamster model, human ApoA1 transgenic mice, pharmacokinetics.

ABSTRACT: BMS-711939 (**3**) is a potent and selective peroxisome proliferator-activated receptor (PPAR) α agonist, with an EC_{50} of 4 nM for human PPARα and >1000-fold selectivity vs. human PPARγ (EC_{50} = 4.5 μM) and PPARδ (EC_{50} > 100 μM) in PPAR-GAL4 transactivation assays. Compound **3** also demonstrated excellent *in vivo* efficacy and safety profiles in preclinical studies and thus was chosen for further preclinical evaluation. The synthesis, structure–activity relationship (SAR) studies, and *in vivo* pharmacology of **3** in preclinical animal models as well as its ADME profile are described.

Peroxisome proliferator-activated receptors (PPARs) are ligand-activated transcription factors in the nuclear hormone receptor superfamily.[1, 2] Three subtypes of PPARs, namely PPARα, PPARγ and PPARδ, have been identified in various species, including humans. PPARα is highly expressed in the liver and regulates the expression of genes encoding lipid and lipoprotein metabolism.[3] Upon binding of PPARα ligand agonists, the resulting conformational change leads to the modulation of a number of PPARα responsive genes, which in turn have pleiotropic effects on plasma lipoprotein levels, atherosclerosis and inflammation. There are currently several synthetic PPARα ligands, including the fibrate class of hypolipidemic drugs in clinical use.[4, 5] Although fibrates are ligands of PPARs, their binding affinity to PPARα is relatively weak.[6, 7] This results in the relatively high doses (e.g. 200 mg of fenofibrate and 1.2 g of gemfibrozil) needed to achieve clinical efficacy, and unwanted side effects may occur at these high doses. Several potent PPARα selective agonists have been progressed into various phases of clinical development, including GW590735[8] and LY518674.[9] However, the development of most of these potent and selective PPARα agonist clinical candidates have been suspended. Recently, the PPARα-selective α,γ dual agonist saroglitazar was approved in India for the treatment of diabetic dyslipidemia.[10] A potent and efficacious PPARα agonist with an excellent safety profile may provide an opportunity for the treatment of atherosclerosis and dyslipidemia as well as non-alcoholic steatohepatitis (NASH)[11] with minimized side effects. In addition, we considered that a more potent and selective PPARα agonist with minimized disparity in interspecies PPAR activities (particularly rodent), will be useful for mechanism-based safety evaluation in preclinical animal models.

Figure 1. Fenofibric acid and BMS-687453

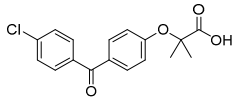

1, Fenofibric Acid

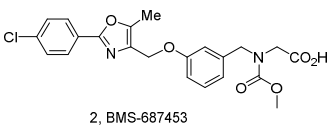

2, BMS-687453

In continuation of our research in the field of PPARs to develop novel therapeutic agents to treat metabolic disorders,[12] we have reported the discovery of the selective PPARα agonist **2**[13] (Figure 1), which exhibited a high degree of selectivity towards PPARα over PPARγ (PPARα EC_{50} = 10 nM, EC_{50} ratio: γ/α = 410), and demonstrated an excellent pharmacological and safety profile in preclinical studies. Inspection of the X-ray crystal structures of **2** bound to the PPARα ligand binding domain (LBD; Figure 2) suggested that the carboxylic acid of **2** forms the well-recognized hydrogen-bonding network with neighboring residues: His440, Tyr464, Tyr314 and Ser280. The 1,3-oxybenzyl central core anchors the acid head group and

the 4-chlorophenyl oxazole moiety into their appropriate binding pockets. Since the central phenyl core and the benzylic carbon are partially surrounded by hydrophobic residues such as Leu321, Ile317 and Phe318, we envioned that small hydrophobic substituents on this region may be tolerated and SAR investigations could be productively conducted within this portion of the molecule to further optimize the binding affinity/potency and/or reduce the human/rodent species difference in PPARα activity. In this paper, we describe the SAR findings from this effort, which resulted in the discovery of **3** (BMS-711939). We also disclose the pharmacokinetic and *in vivo* efficacy profiling of **3**, which progressed into preclinical toxicology studies.

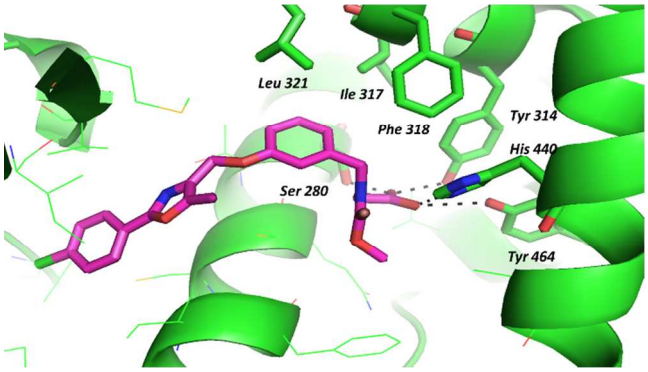

Figure 2. X-ray crystal structure of **2** bound in PPARα LBD with 2.7Å resolution. Residues within 4.5 Å of benzylglycine are shown with thick sticks. Hydrogen bonds are shown as black dashed lines. The PDB deposition number is 3KDT.

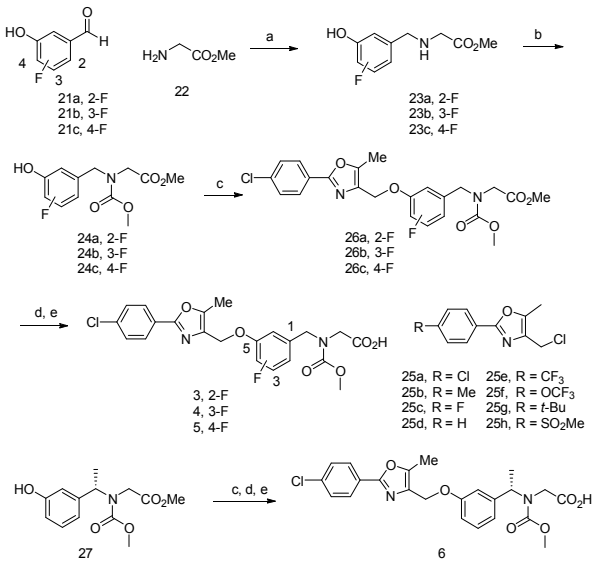

Scheme 1. The synthesis of **3-6**. Reagents and conditions: (a) Et_3N, MeOH, $NaBH_4$, 0°C to rt. (b) methyl chloroformate, aq. $NaHCO_3$, THF. (c) **25a**, K_2CO_3, MeCN, 80°C. (d) LiOH, THF-H_2O, rt. (e) 1N aq. HCl.

The syntheses of **3-6** are described in Scheme 1. Reductive amination of fluoro-substituted hydroxybenzaldehydes **21a-c** with glycine methyl ester hydrochloride **22** afforded the secondary amines **23a-c** in 85-95% yield. Reaction of **23a-c** with methyl chloroformate gave the corresponding methyl carbamates **24a-c** in 90-99% yield. Base-mediated alkylation of phenols **24a-c** with 4-(chloromethyl)-2-(4-chlorophenyl)-5-methyloxazole **25a** at 80°C provided the methyl esters **26a-c** in 86-99% yield. Basic hydrolysis of **26a-c** provided **3-5** in 90-93% yield. Compound **6** was synthesized in a similar fashion from intermediate **27**.[14] Compounds **7-13** were synthesized from intermediate **24a** and oxazoles **25b-h**[15] using the same synthetic sequence as described for **3-5**.

Compounds **14-20** were synthesized through a slightly different sequence as shown in Scheme 2. Alkylation of 2-fluoro-5-hydroxybenzaldehyde **21a** with 4-(chloromethyl) oxazole **25a** provided aldehyde **28** in 95% yield. Reductive amination of **28** with **22** afforded the secondary amine **29** in 90% yield. Reaction of **29** with different chloroformates and subsequent hydrolysis of the resulting esters provided compound**s 14-20** in 80-93% yield.

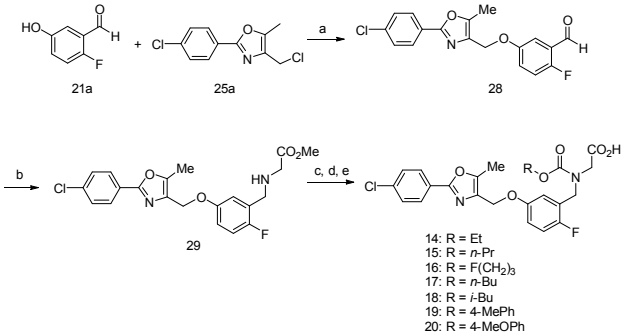

Scheme 2. The synthesis of **14-20**. Reagents and conditions: (a) K_2CO_3, MeCN, 80°C. (b) **22**, Et_3N, MeOH, $NaBH_4$, 0°C to rt. (c) ROCOCl, aq. $NaHCO_3$, THF. (d) LiOH, THF-H_2O, rt. (e) 1N aq. HCl.

Our initial effort to further optimize **2** focused on structural modifications of the central core and the benzylic position of the benzylglycine. The SAR results are shown in Table 1. Introducing a fluorine atom at the 2-position of central core resulted in a very potent and selective PPARα/γ agonist **3** (EC_{50} γ/α ratio = 1128), with PPARα EC_{50} = 4 nM and PPARγ EC_{50} = 4.51 μM in the transactivation assays.[13] This compound is ~2.5-fold more potent than **2** (EC_{50} = 10 nM) at PPARα, and is slightly less potent at PPARγ than **2** (PPARγ EC_{50} = 4.1 μM). These functional data correspond well to their PPARα and PPARγ binding affinities (Table 1).[16] On the other hand, the opposite effects were observed when introducing a fluorine atom at the 3-position of central phenyl core; compound **4** (EC_{50} γ/α ratio = 157) is less potent at PPARα (EC_{50} = 18 nM) and more potent at PPARγ (EC_{50} = 2.82 μM) than **2**. Interestingly, the 4-fluoro-substituted analog **5** is less active than **2** at both PPARα and PPARγ with a γ/α EC_{50} ratio of 98. When a (S)-methyl group is placed at the α-position of the benzylglycine of **2**, the resulting **6** (EC_{50} γ/α ratio = 332) has similar potency at PPARα but is more potent at PPARγ than **2**. These results indicate that a subtle substitution change on the central phenyl core or at the benzylic position can result in changes in both the PPARα and PPARγ agonist activities and thus the PPARγ/α selec-

tivety. The 2-fluorophenyl glycine analog **3** has the most potent PPARα agonist activity and is also the most selective PPARα agonist among the three isomeric monofluorinated analogs.

Table 1. Transactivation EC_{50} and binding IC_{50} of 2-6[a]

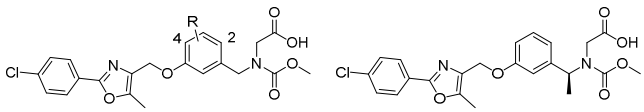

Cpd	R	αEC50 (nM)	γEC50 (nM)	γ/α EC50 ratio	αIC50 (nM)	γIC50 (nM)
2	H	10	4096	410	260	>48000
3	2-F	4.0	4511	1128	97	>98400
4	3-F	18	2819	157	1341	>15000
5	4-F	94	9168	98	1563	>15000
6	-	8.6	2857	332	671	>15000

[a] Compounds were tested for agonist activity on hPPAR-GAL4 HEK transactivation assay. Transactivation efficacy was defined as percentage of maximum activity as compared with an appropriate standard set at 100% (100 μM fenofibric acid for PPARα, 1.0 μM rosiglitazone for PPARγ). Full PPARα intrinsic activity (>50% relative to 100 μM fenofibric acid) was observed for all tested compounds (n = 1-3).

With lead compound **3** in hand, we systematically investigated the SAR of the "left-hand" phenyl ring substituents and the "right-hand" carbamate substituents, as shown in Table 2. In general, all the 2-fluoro-phenyl central core based compounds show enhanced PPARα agonist activity and PPARα/γ selectivity versus their corresponding unsubstituted phenyl analogs.[13] On the "left-hand" phenyl ring (of the oxazole), while the compound without a *para* substituent (**9,** PPARα EC_{50}= 59 nM, γ/α ratio = 146) is ~15-fold less potent and far less selective than **3**, the *para*-fluoro compound **8** is only about 3.5-fold less potent than **3** at PPARα and maintains high selectivity (PPARα EC_{50}= 15 nM, γ/α ratio = 691). Compounds with a non-polar substituent (**7, 10-12**) at the *para* position generally have similar PPARα potencies to **3**. On the other hand, the relatively bulky polar methylsulfonyl substituent (**13**) obliterates both PPARα and γ activities. Interestingly, a bulky aliphatic substituent such as *t*-butyl (**12**) significantly improved PPARγ potency while maintaining PPARα activity, thus resulting in a significant reduction in PPARα selectivity versus **3**. These results suggested that polarity and steric effects play important roles in determining PPARα/γ functional activities and selectivity in this portion of the molecule. This SAR study of the "left-hand" phenyl ring substituents showed that the 4-Cl-phenyl moiety was optimal, providing potent PPARα activity and the highest level of PPARα selectivity.

The corresponding SAR study of the "right-hand" side carbamate showed that simple alkyl carbamates (**14-20**) generally provide excellent PPARα potency and selectivity (EC_{50} γ/α ratio > 400-fold), with the ethyl carbamate **14** having almost the same PPARα potency and selectivity (PPARα EC_{50}= 4 nM, γ/α ratio = 1085) as **3**. Interestingly, replacing the terminal methyl group of the *n*-propyl carbamate **15** with a fluoromethyl (**16**) resulted in a >2-fold decrease in potency at both PPARα and γ, but retained the high γ/α selectivity ratio. The aryl carbamates (**19** & **20**) were also potent PPARα agonists, but with slightly lower γ/α selectivity compared to the simple alkyl carbamates. The overall SAR in this carbamate region is similar to that previously observed with **2,** with the methyl carbamate being optimal.[13]

Cpd	R^1	R^2	αEC50 (nM)	γEC50 (nM)	γ/α Ratio
3	4-Cl	Me	4.0	4511	1128
7	4-Me	Me	2.8	2182	787
8	4-F	Me	14.5	10010	691
9	4-H	Me	59	8607	146
10	4-CF_3	Me	3.6	2062	566
11	4-CF_3O	Me	4.3	2384	556
12	4-$C(CH_3)_3$	Me	2.7	414	154
13	4-$MeSO_2$	Me	>2500	>25000	NA
14	4-Cl	Et	4.0	4273	1085
15	4-Cl	*n*-Pr	3.4	2013	594
16	4-Cl	$F(CH_2)_3$	10.6	4383	413
17	4-Cl	*n*-Bu	2.8	1235	435
18	4-Cl	*i*-Bu	2.3	1504	666
19	4-Cl	4-MePh	5.6	1255	224
20	4-Cl	4-MeOPh	6.8	1087	160

Table 2. *In vitro* activity of 2-fluoro substituted benzylglycine 3, 7-20[a]

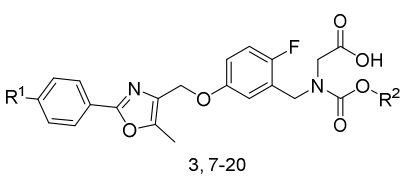

[a] See notes for Table 1.

The PPARα potency and selectivity of **3** were further confirmed by testing it in co-transfection assays in HepG2 cells using full length human PPARα and PPARγ receptors.[13] In these assays, compound **3** showed excellent PPARα potency (EC_{50} = 5 nM) with > 320-fold selectivity vs. PPARγ (EC_{50} > 1.61 μM). These results correlated well with the data observed from the primary GAL-4 HEK transactivation based screening assays as shown in Table 1. Compound **3** also is a full PPARα agonist in the rodent assays, and is > 2.5-fold more potent than **2** in rodent PPARα functional assays, with EC_{50}s of 178 nM, 144 nM and 123 nM for hamster, mouse and rat, respectively.[17] Importantly, compound **3** showed negligible activity (EC_{50} for transactivation >25 μM and efficacies <15% of standard) against a panel of human nuclear hormone receptors, including PPARδ, LXR, GR and RXR.

Compound **3** did not show any significant activity in liability profiling assays (e.g. in 5 human CYP isozymes, PXR and hepatocyte toxicity assays).[18] No *in vitro* liabilities were noted in: 1) extensive screens for receptor/enzyme binding inhibition; 2) assays for bacterial mutagenicity or CHO cell clastogenicity and 3) an exploratory Ames test at up to 5000 μg per plate in TA98 and TA100 strains. Cardiovascular safety evaluations were carried out on **3**: 1) no hERG and sodium channel activity was observed at concentrations up to 30 μM and 10 μM, respectively; and 2) no drug-related changes in hemodynamic and electrocardiographic (ECG) effects were observed at up to 20 mg/kg of **3** in a single-dose monkey telemetry study.

Compound **3** also exhibited an excellent pharmacokinetic profile across all tested animal species. Table 3 shows the pharmacokinetic parameters of **3** in mouse, rat, dog and monkey (cynomulgus). It exhibited low plasma clearance in the mouse, rat, and monkey, and moderate plasma clearance in the dog. The half-life of ranged from 1.8 h in mouse to 26.3 h in monkey. It also had excellent absolute oral bioavailability ranging from 59% (dog) to 100% (rat). Additionally, it has excellent crystalline aqueous solubility (367 μg/mL at pH 7.2).

Compound **3** has been profiled in multiple animal models of dyslipidemia.[19] In a 10-day dose response study in the human ApoA1 transgenic mouse,[20] it robustly and dose-dependently increased both ApoA1 and HDL cholesterol, as shown in Table 4. In this study, the reference compound fenofibrate (at a dose of 100 mg/kg) raised serum HDL cholesterol by 88% and lowered triglycerides by 33% after 10 days of dosing. By comparison, compound **3** (at a dose of 50 mg/kg/day) raised HDL cholesterol by 109% and lowered triglycerides by 59% respectively. These data clearly demonstrated that **3** robustly elevated HDLc and lowered triglycerides in the human ApoA1 transgenic mouse model.

In a 21-day head-to-head comparison study in a high fat fed hamster model,[21] both **2** and **3** dose dependently lowered triglycerides and LDL levels. As shown in Table 5, after three weeks of dosing, compound **3** lowered fasting plasma LDLc by 61% at the 3 mg/kg/day dose and 87% at the 10 mg/kg/day dose respectively; it also reduced plasma triglycerides by 50%, 74% and 85% at the 1, 3 and 10 mg/kg/day doses, respectively. In comparison, compound **2** lowered fasting plasma LDLc by 46% at the 3 mg/kg/day dose and 60% at the 10 mg/kg/day dose respectively; it reduced plasma triglycerides by 40%, 45% and 77% at the 1, 3 and 10 mg/kg/day doses, respectively. For liver triglycerides and cholesterol, compound **3** lowered liver cholesterol by 57% at the 3 mg/kg/day dose and 68% at the 10 mg/kg/day dose respectively; it also reduced liver triglycerides by 19%, 40% and 48% at the 1, 3 and 10 mg/kg/day doses, respectively. By comparison, compound **2** only impacted the hepatic lipids at the 10 mg/kg dose level (41% for liver cholesterol and 23% for liver triglycerides). Overall, compound **3** significantly lowered plasma triglycerides and LDLc in a chronic dyslipidemic hamster model, and compares favorably to **2** in terms of both potency and overall efficacy in lipid lowering in this model.

In summary, the SAR investigation on the oxybenzylglycine-based lead **2** led to the discovery of a series of 2-flouro-substituted benzylglycine analogs as potent and highly selective PPARα agonists. BMS-711939 (**3**) was found to be a potent and highly selective PPARα agonist (PPARα EC_{50} = 4 nM, EC_{50} γ/α ratio = 1128) that is highly efficacious in elevating HDLc in human ApoA1 transgenic mice and lowering LDLc in dyslipidemic hamsters in chronic efficacy studies. It also robustly lowers triglycerides in both of these animal models. In comparison to the **2**, BMS-711939 is more potent at PPARα and more selective against PPARγ, and shows superior potency on lowering LDLc and TG in hamsters. On the basis of its potency and selectivity, its excellent *in vitro* liability profile, favorable pharmacokinetics and pharmacodynamic effects in animal models, compound **3** was selected for further evaluation in preclinical animal toxicity studies.

Table 3. Pharmacokinetic profile of 3[a]

Species	Dose route	Dose (mg/kg)	t_{max} (h)	C_{max} (μM)	AUC[b] (μM·h)	CL_{Pl} (mL/min/kg)	V_{SS} (L/kg)	$t_{1/2}$ (h)	F%
Mouse	IV	5	-	-	13	13.8	0.6	1.8	-
	PO	10	0.25	22.7	17	-	-	-	66

Rat	IV	4	-	-	9.4	15.3 ± 0.7	2.2 ± 0.5	3.3	-
	PO	8	0.3 ± 0.1	14.9	32	-	-	-	100
Dog	IV	1	-	-	3.5	10.7 ± 2.4	2.1 ± 1.2	5.5	-
	PO	2	0.8 ± 0.3	1.5	4.0	-	-	-	59
Monkey	IV	1	-	-	7.5	5.9 ± 2.7	3.9 ± 1.5	26.3	-
	PO	2	0.9 ± 0.1	1.4	8.5	-	-	-	65

[a]For each experimental study, n ≥ 3. [b]$AUC_{0\text{-}8h}$ reported here, not $AUC_{INF.}$

Table 4: Effect of 3 and fenofibrate on plasma parameters in human ApoA1 transgenic mice[a]

Entry	Liver TG mg/dL ± SEM (% change)	Liver chol mg/dL ± SEM (% change)	Plasma LDLc mg/dL ± SEM (% change)	Plasma TG mg/dL ± SEM (% change)
High Fat Vehicle	24.1 ± 1.5	16.9 ± 1.2	91.7 ± 8.1	173.5 ± 17
3, 10 mg/kg	12.5 ± 1.2 (-48%*)	5.5 ± 0.5 (-67.5%*)	12.2 ± 4.6 (-87%*)	25.2 ± 2.6 (-85%*)
3 mg/kg	14.5 ± 0.8 (-39.8%*)	7.3 ± 0.7 (-56.8%*)	35.7 ± 4.5 (-61%*)	44.7 ± 4.3 (-74%*)
1 mg/kg	19.6 ± 0.9 (-18.7%*)	14.7 ± 1.9 (-13%)	69.3 ± 11 (-24%)	85.7 ± 18 (-50%*)
2, 10 mg/kg	18.5 ± 1.2 (-23%*)	10.0 ± 1.0 (-40.8%*)	36.3 ± 5.7 (-60%*)	39.7 ± 3.6 (-77%*)
3 mg/kg	19.9 ± 3.0 (-17%)	14.3 ± 2.4 (-15.4%)	49.9 ± 8.4 (-46%*)	95.2 ± 13 (-45%*)
1 mg/kg	22.6 ± 1.1 (-6%)	20.7 ± 2.1 (+22%)	89.3 ± 9.4	103.2 ± 11 (-40%*)

[a]$p < 0.05$ compared to vehicle-treated group (n = 10). Data represent the mean ± SEM (n=10).

Table 5: Effect of compounds 2 and 3 on lipid parameters in high fat-fed hamsters[a]

Entry	Liver TG mg/dL ± SEM (% change)	Liver chol mg/dL ± SEM (% change)	Plasma LDLc mg/dL ± SEM (% change)	Plasma TG mg/dL ± SEM (% change)
High Fat Vehicle	24.1 ± 1.5	16.9 ± 1.2	91.7 ± 8.1	173.5 ± 17
3, 10 mg/kg	12.5 ± 1.2 (-48%*)	5.5 ± 0.5 (-67.5%*)	12.2 ± 4.6 (-87%*)	25.2 ± 2.6 (-85%*)
3 mg/kg	14.5 ± 0.8 (-39.8%*)	7.3 ± 0.7 (-56.8%*)	35.7 ± 4.5 (-61%*)	44.7 ± 4.3 (-74%*)
1 mg/kg	19.6 ± 0.9 (-18.7%*)	14.7 ± 1.9 (-13%)	69.3 ± 11 (-24%)	85.7 ± 18 (-50%*)
2, 10 mg/kg	18.5 ± 1.2 (-23%*)	10.0 ± 1.0 (-40.8%*)	36.3 ± 5.7 (-60%*)	39.7 ± 3.6 (-77%*)
3 mg/kg	19.9 ± 3.0 (-17%)	14.3 ± 2.4 (-15.4%)	49.9 ± 8.4 (-46%*)	95.2 ± 13 (-45%*)
1 mg/kg	22.6 ± 1.1 (-6%)	20.7 ± 2.1 (+22%)	89.3 ± 9.4	103.2 ± 11 (-40%*)

[a]p <0.05 versus vehicle control. Data represent the mean ± SEM (n=8).

ASSOCIATED CONTENT

Supporting Information

The Supporting Information is available free of charge on the ACS Publications website at DOI: XXX.

Synthetic methods, characterization of key compounds, and biology assay protocols (PDF).

AUTHOR INFORMATION

Corresponding Author

* Tel: 1-609-466-5076. E-mail: yan.shibms.com

Notes

The authors declare no competing financial interest.

ACKNOWLEDGMENT

We thank Dr. Jeff Robl for careful proofreading of this manuscript. The Discovery Toxicology department at Bristol-Myers Squibb is acknowledged for the preclinical safety evaluation of BMS-711939.

ABBREVIATIONS

Peroxisome Proliferator Activated Receptor (PPAR); ligand binding domain (LBD); low-density lipoprotein-cholesterol (LDLc); high-density lipoproteincholesterol (HDLc); triglycerides (TG); Cytochromes P450 (CYP); Human Ether-à-go-go-Related Gene (hERG); Liver X Receptor (LXR); Glucocor-

ticoid Receptor (GR); Pregnane X Receptor (PXR); Retinoid X Receptor RXR.

REFERENCES

1. Pirat, C.; Farce, A.; Lebègue, N.; Renault, N.; Furman, C.; Millet, R.; Yous, S.; Speca, S.; Berthelot, P.; Desreumaux, P.; Chavatte, P. Targeting peroxisome proliferator-activated receptors (PPARs): development of modulators. *J. Med. Chem.* **2012**, *55*, 4027-4061.
2. Cheng, P. T. W.; Mukherjee, R. PPARs as targets for metabolic and cardio-vascular diseases. *Mini-Rev. Med. Chem*. **2005**, *5*, 741-753.
3. Staels, B.; Dallongeville, J.; Auwerx; J.; Schoonjans, E.; Leitersdorf, E.; Fruchart, J.-C. Mechanism of action of fibrates on lipid and lipoprotein metabolism. *Circulations*, **1998**, *98*, 2088-2093.
4. Saurav, A.; Kaushik, M.; Mohiuddin, S. M. Fenofibric acid for hyperlipidemia. *Exp. Opin. Pharmacother*. **2012**, *13*, 717-722.
5. Todd, P. A.; Ward, A. Gemfibrozil. A review of its pharmacodynamic and pharmacokinetic properties, and therapeutic use in dyslipidaemia. *Drugs* **1988**, *36*, 314-339.
6. Dietz, M.; Mohr, P.; Kuhn, B.; Maerki, H. P.; Hartman, P.; Ruf, A.; Benz, J.; Grether, U.; Wright, M. B. Comparative molecular profiling of the PPARα/γ activator aleglitazar: PPAR selectivity, activity and interaction with cofactors. *ChemMedChem*. **2012**, *7*, 1101-1011.
7. Forman, B. M.; Chen, J.; Evans, R. M. Hypolipidemic drugs, polyunsaturated fatty acids, and eicosanoids are ligands for peroxisome proliferator-activated receptors alpha and delta. *Proc. Natl. Acad. Sci. U.S.A*. **1997**, *94*, 4312-4317.
8. Sierra, M. L.; Beneton, V.; Boullay, A-B.; Boyer, T.; Brewster, A. G.; Donche, F.; Forest, M-C.; Fouchet, M-H.; Gellibert, F. J.; Grillot, D. A.; Lambert, M. H.; Laroze, A.; Le Grumelec, C.; Linget, J. M.; Montana, V. G.; Nguyen, V-L.; Nicodeme, E.; Patel, V.; Penfornis, A.; Pineau, O.; Pohin, D.; Potvain, F.; Poulain, G.; Ruault, C. B.; Saunders, M.; Toum, J.; Xu, H. Eric; Xu, R. X.; Pianetti, P. M. Substituted 2-[(4-aminomethyl)phenoxy]-2-methylpropionic acid PPARalpha agonists. 1. Discovery of a novel series of potent HDLc raising agents. *J. Med. Chem.* **2007**, *50*, 685-695.
9. Xu, Y.; Mayhugh, D.; Saeed, A.; Wang, X.; Thompson, R. C.; Dominianni, S. J.; Kauffman, R. F.; Singh, J.; Bean, J. S.; Bensch, W. R.; Barr, R. W.; Osborne, J.; Montrose-Rafizadeh, C.; Zink, R. W.; Yumibe, N. P.; Huang, N.; Luffer-Atlas, D.; Rungta, D.; Maise, D. E.; Mantlo, N. B. Design and Synthesis of a Potent and Selective Triazolone-Based Peroxisome Proliferator-Activated Receptor α Agonist. *J. Med. Chem.* **2003,** *46*, 5121-5124.
10. Sosale, A.; Saboo, B.; Sosale B. *Diabetes Metab Syndr Obes.* **2015,** *8*, 189-196.
11. Pawlak, M.; Lefebvre, P.; Staels, B. Molecular mechanism of PPARα action and its impact on lipid metabolism, inflammation and fibrosis in non-alcoholic fatty liver disease. *J. Hepatol*. **2015**, *62*, 720-733.
12. Devasthale, P. V.; Chen, S.; Jeon, Y.; Qu, F.; Shao, C.; Wang, W.; Zhang, H.; Farrelly, D.; Golla, R.; Grover, G.; Harrity, T.; Ma, Z.; Moore, L.; Ren, J.; Seethala, R.; Cheng, L.; Sleph, P.; Sun, W.; Tieman, A.; Wetterau, J. R..; Doweyko, A.; Chandrasena, G.; Chang, S. Y.; Humphreys, W. G.; Sasseville, V. G.; Biller, S. A.; Ryono, D. E.; Selan, F.; Hariharan, N.; Cheng, P. T. W. Design and Synthesis of N-[(4-Methoxyphenoxy)carbonyl]-N-[[4-[2-(5- methyl-2-phenyl-4-oxazolyl)ethoxy]phenyl]methyl]glycine [Muraglitazar/BMS-298585], a Novel Peroxisome Proliferator-Activated Receptor α/γ Dual Agonist with Efficacious Glucose and Lipid-Lowering Activities. *J. Med. Chem.* **2005**, *48*, 2248-2250.
13. Li, J.; Kennedy, L. J.; Shi, Y.; Tao, S.; Ye, X.-Y.; Chen, S. Y.; Wang, Y.; Hernández, A. S.; Wang, W.; Devasthale, P. V.; Chen, S.; Lai, Z.; Zhang, H.; Wu, S.; Smirk, R. A.; Bolton, S. A.; Ryono, D. E.; Zhang, H.; Lim, N.-K.; Chen, B.-C.; Locke, K. T.; O'Malley, K. M.; Zhang, L.; Srivastava, R. A.; Miao, B.; Meyers, D. S.; Monshizadegan, H.; Search, D.; Grimm, D.; Zhang, R.; Harrity, T.; Kunselman, L. K.; Cap, M.; Kadiyala, P.; Hosagrahara, V.; Zhang, L.; Xu, C.; Li, Y.-X.; Muckelbauer, J. K.; Chang, C.; An, Y.; Krystek, S. R.; Blanar, M. A.; Zahler, R.; Mukherjee, R.; Cheng, P. T. W.; Tino, J. A. Discovery of an Oxybenzylglycine Based Peroxisome Proliferator Activated Receptor α Selective Agonist 2-((3-((2-(4-Chlorophenyl)-5-methyloxazol-4-yl)methoxy)benzyl)(methoxycarbonyl)-amino)acetic Acid (BMS-687453). *J. Med. Chem*. **2010**, *53*, 2854–2864.
14. Ye, X.-Y.; Chen, S. Y.; Zhang, H.; Locke, K. T.; O'Malley, K.; Zhang, L.; Srivastava, R. A.; Miao, B.; Meyers, D. S.; Monshizadegan, H.; Search, D.; Grimm, D.; Zhang, R.; Lippy, S. J.; Twamley, C.; Muckelbauer, J. K.; Chang, C.; An, Y.; Hosagrahara, V.; Zhang, L.; Yang, T-J., Mukherjee, R.; Cheng, P. T. W.; Tino, J. Synthesis and structure–activity relationships of 2-aryl-4-oxazolylmethoxybenzylglycines and 2-aryl-4-thiazolylmethoxy benzylglycines as novel, potent PPARα selective activators- PPARα and PPARγ selectivity modulation. *Bioorg. Med. Chem. Lett***. 2010**, *20*, 2933-2937.
15. Zhang, H.; Yan, P. F.; Zhang, G-L. Preparation of 2-(1-Chloroalkyl)-4,5-dimethyloxazoles and (*E*)-2-Alkenyl-4,5-dimethyloxazoles. *Synthesis* **2006**, *11*, 1763-1766.
16. Seethala, R.; Golla, R.; Ma, Z.; Zhang, H.; O'Malley, K.; Lippy, J.; Cheng, L.; Mookhtiar, K.; Farrelly, D.; Zhang, L.; Hariharan, N.; and Cheng. P. T. A rapid, homogeneous, fluorescence polarization binding assay for peroxisome proliferator-activated receptors alpha and gamma using a fluorescein-tagged dual PPARalpha/gamma activator. *Anal. Biochem.* **2007**, *363*, 263-274.
17. Compound **2** shows full PPARα agonist activity in rodents with EC_{50}s of 488 nM, 426 nM and 317 nM for hamster, mouse and rat, respectively.
18. Compound **3** has following profile: Plasma Protein binding: 99.7% (h), 99.8% (m), 99.6% (r), 99% (c), 99.5% (d); CYP (inhibition) 3A4, 1A2, 2B6, 2C8, 2C9, 2C19, 2D6, all IC_{50}s > 40 μM. PXR EC_{60} > 50 μM; HHA (2C19, 2C9, 2D6, 3A4, TC5) all IC_{50} > 150 μM; hERG (flux) IC_{50} > 80 μM; (patch-clamp) 4.0% at 30 μM; Sodium Channel (EP, % block @ 10 μM): 12% @ 1 Hz and 14% @ 4 Hz; Purkinje fiber% change APD_{90} = -5.4 @ 30 μM.
19. Mukherjee, R.; Locke, K. T.; Miao, B.; Meyers, D.; Monshizadegan, H.; Zhang, R.; Search, D.; Grimm, D.; Flynn, M.; O'Malley, K. M.; Zhang, L.; Li, J.; Shi, Y.; Kennedy, L. J.; Blanar, M.; Cheng, P. T.; Tino, J. A.; Srivastava, R. A. Novel Peroxisome Proliferator-Activated Receptor α Agonists Lower Low-Density Lipoprotein and Triglycerides, Raise High-Density Lipoprotein, and Synergistically Increase Cholesterol Excretion with a Liver X Receptor Agonist. *J. Pharmacol. Exp. Ther.* **2008**, *327*, 716-726.
20. Berthou, L.; Duverger, N.; Emmanuel., F.; Langouët, S.; Auwerx, J.; Guillouzo, A.; Fruchart, J. C.; Rubin, E.; Denèfle, P.; Staels, B.; Branellec, D. Opposite Regulation of Human Versus Mouse Apolipoprotein A-I by Fibrates in Human Apolipoprotein A-I Transgenic Mice. *J. Clin. Invest*. **1996**, *97*, 2408-2416.
21. Wang, P.R.; Guo, Q.; Ippolito, M.; Wu, M.; Milot, D.; Ventre, J.; Doebber, T.; Wright, S. D.; Chao, Y. S. High fat fed hamster, a unique animal model for treatment of diabetic

dyslipidemia with peroxisome proliferator activated receptor alpha selective agonists. *Eur. J. Pharmacol.* **2001**, *427*, 285-293.

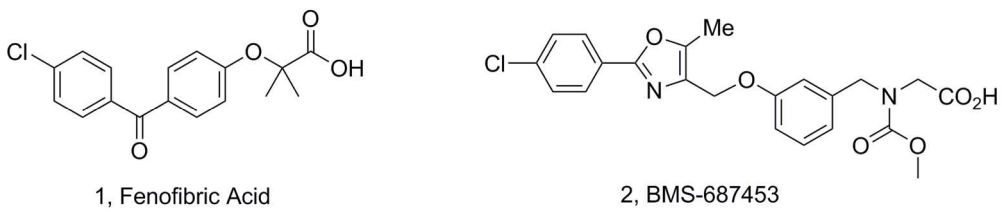

Figure 1. Fenofibric Acid and BMS-687453
154x32mm (300 x 300 DPI)

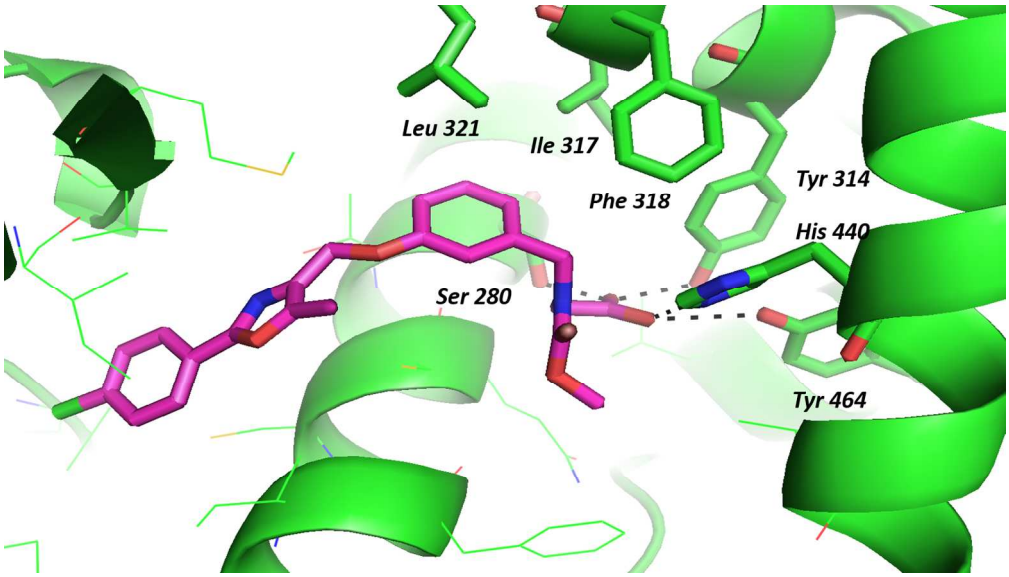

Figure 2. X-ray crystal structure of compound **2** bound in PPARα LBD with 2.7Å resolution. Residues within 4.5 Å of benzylglycine are shown with thick sticks. Hydrogen bonds are shown as black dashed lines. The PDB deposition number is 3KDT.
287x162mm (150 x 150 DPI)

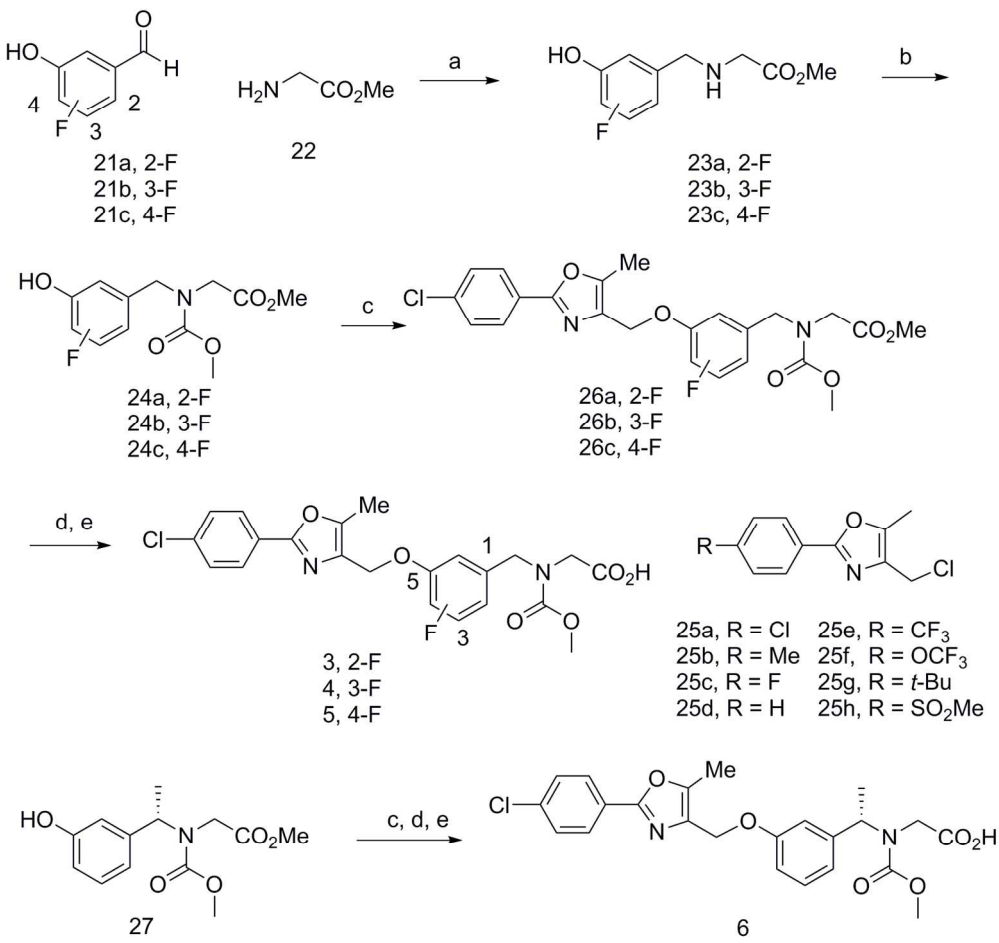

Scheme 1. The synthesis of **3-6**. Reagents and conditions: (a) Et_3N, MeOH, $NaBH_4$, 0°C to rt. (b) methyl chloroformate, aq. $NaHCO_3$, THF. (c) **25a**, K_2CO_3, MeCN, 80°C. (d) LiOH, THF-H_2O, rt. (e) 1N aq. HCl.
156x147mm (300 x 300 DPI)

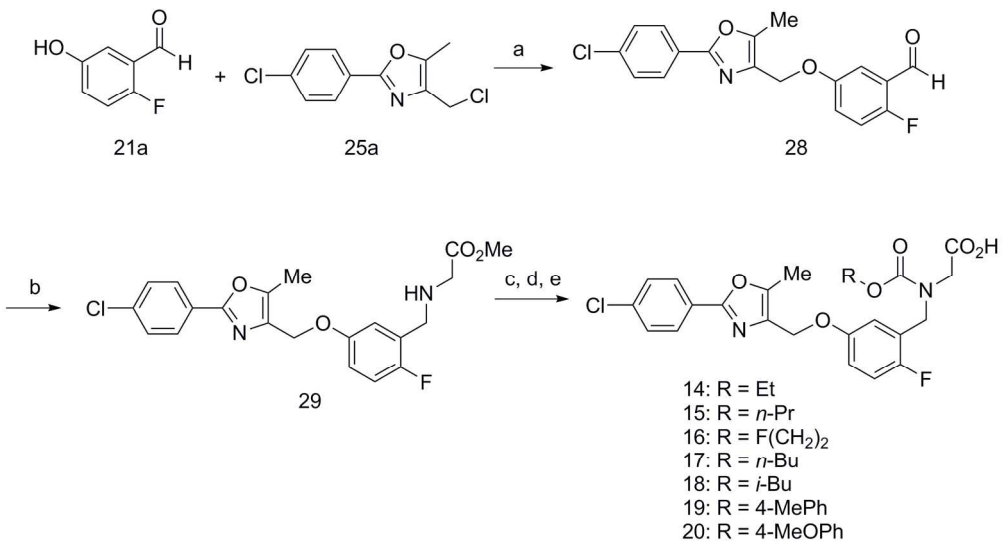

Scheme 2. The synthesis of **14-20**. Reagents and conditions: (a) K_2CO_3, MeCN, 80°C. (b) **22**, Et_3N, MeOH, $NaBH_4$, 0°C to rt. (c) ROCOCl, aq. $NaHCO_3$, THF. (d) LiOH, THF-H_2O, rt. (e) 1N aq. HCl.
170x93mm (300 x 300 DPI)

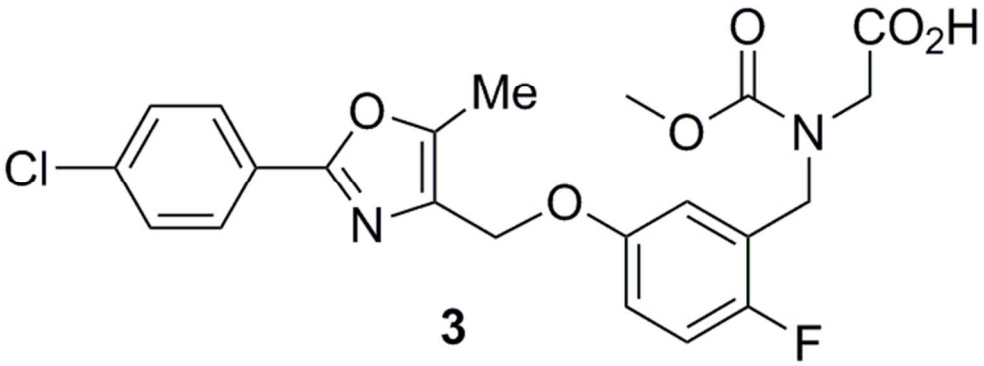

3

PPARα EC_{50} = 4.0 nM

PPARγ EC_{50} = 4511 nM

PPARδ EC_{50} > 100 μM

Discovery and Preclinical Evaluation of BMS-711939, an Oxybenzyl-glycine Based PPARα Selective Agonist

Yan Shi,* Jun Li, Lawrence J. Kennedy, Shiwei Tao, Andrés S. Hernández, Zhi Lai, Sean Chen, Henry Wong, Juliang Zhu, Ashok Trehan, Ngiap-Kie Lim, Huiping Zhang, Bang-Chi Chen, Kenneth T. Locke, Kevin M. O'Malley, Litao Zhang, Raiajit Srivastava, Bowman Miao, Daniel S. Meyers, Hossain Monshizadegan, Debra Search, Denise Grimm, Rongan Zhang, Thomas Harrity, Lori K. Kunselman, Michael Cap, Jodi Muckelbauer, Chiehying Chang, Stanley R. Krystek, Yi-Xin Li, Vinayak Hosagra-hara, Lisa Zhang, Pathanjali Kadiyala, Carrie Xu, Michael A. Blanar, Robert Zahler, Ranjan Mukherjee, Peter T. W. Cheng, Joseph A. Tino

60x34mm (300 x 300 DPI)